# Partial power DC-DC converter for large-scale photovoltaic systems

Jaime Zapata, Thierry Meynard, Samir Kouro

# Partial Power DC-DC Converter for Large-Scale Photovoltaic Systems

Jaime W. Zapata*, Thierry A. Meynard† and Samir Kouro*
*Electronics Engineering Department, Universidad Tecnica Federico Santa Maria, Valparaiso, Chile
†Institut National Polytechnique de Toulouse, University of Toulouse, Toulouse, France
Email: jaime.zapataa.13@sansano.usm.cl, samir.kouro@ieee.org

In photovoltaic (PV) systems, a wide variety of power converter topologies and PV configurations have been developed in order to increase the system efficiency. Traditionally, grid-connected PV systems use one or two conversion stages. The single conversion stage is mainly used for large-scale PV systems working with only a DC-AC converter. Whereas, for small and medium-scale, two conversion stages are used. The advantages working with a DC-stage are mainly the distributed maximum power point tracking (MPPT) algorithm and the elevation capa-bility, but it presents a reduced conversion efficiency compared with the single stage configurations. On the other hand, the single conversion stage presents a reduced overall efficiency produced by partial shading. The proposed work presents a Partial Power DC-DC converter (PPC) which process only a portion of the whole power, reducing the conversion losses. It includes the benefits of two stage configurations so that it performs individual MPPT. Besides, due to the modularity of the architecture, it allows the parallel connection of many strings as required to use in large-scale PV systems. Simulations are performed in order to evaluate the converter performance.

## I. Introduction

Energy production through solar photovoltaic (PV) panels has experienced a significant growth given that it has become cost-competitive compared with fossil-fuel based solutions. During 2014 the global installed power increased around 29% compared with the previous year, reaching a total of 177GW [1].

Traditionally, a PV panel has a low output voltage which is not high enough to perform grid-connection directly. The large-scale PV systems work with series connected modules to reach the required voltage for the grid-connection. The Maximum Power Point Tracking (MPPT) voltage typically vary between 550-850V (a string may not surpass 1000V) [2]. Therefore, the voltage elevation stage is not required and the MPPT algorithm is performed by the inverter stage.

The traditional solution working with large-scale PV systems is the central configuration. It has a three-phase inverter injecting power into grid from a large PV system. It is the simplest and commercially cheaper configuration, besides it has a high conversion efficiency. Despite of the advantages, this configuration has the lowest MPPT capabilities [3].

When a DC-stage is included to the system, it is named as a two stage configuration, but they are commonly used in small and medium scale PV systems [4]. The two stage configurations are suitable to perform distributed MPPT algorithms, because they allow an independent control of the voltage per string, reaching higher energy yields in the case of partial shading [5].

In this paper, a two stage architecture for large-scale PV system is proposed. Based on the concept of partial power converter (PPC), a non-isolated DC-DC converter is used to perform independent input voltage control, which is required to extract the maximum power per each PV string.

## II. Partial power converters

Due to the additional stage, the conversion efficiency presented in two stage configurations is lower compared with the single stage architectures. In order to overcome the low efficiency, some authors have proposed different solutions working with interleaved configurations [6], or reducing the conversion losses by using topologies with lower rates of the power electronic switches [7]. In this case, a floating capacitor is used to fix the converter voltage in a reduced value compared with the total input voltage.

The concept of partial power converter has been presented in [8], [9], which uses isolated converters in order to make the connection, avoid a short circuit and elevate the input voltage. However, actually they are used only for small scale PV systems. The technique of partial power processing, where only a portion of the total power is handled by the converter, can significantly reduce the size and power losses of the converter [10], [11]. In order to analyze the power processed by the converter, a variable called partial power ratio $K_{pr}$ is established as,

$$K_{pr} = \frac{P_{pc}}{P_{pv}}, \tag{1}$$

where, $P_{pc}$ and $P_{pv}$ are the power processed by the converter and the power delivered by the PV system respectively. It means that the converter is considered as PPC when the power ratio is lower than unity, $K_{pr} < 1$.

## III. Proposed power converter

### A. Topology description

The proposed solution is based on a series converter which works as an interface between the PV system and the DC-link as shown in Fig. 1. It comprises a half-bridge converter per PV string and an input inductor $L_n(n = \{1, 2, 3\})$. All of them share the floating capacitor $C_{pc}$ and the half-bridge connected to the DC-link. Due to the modular design,

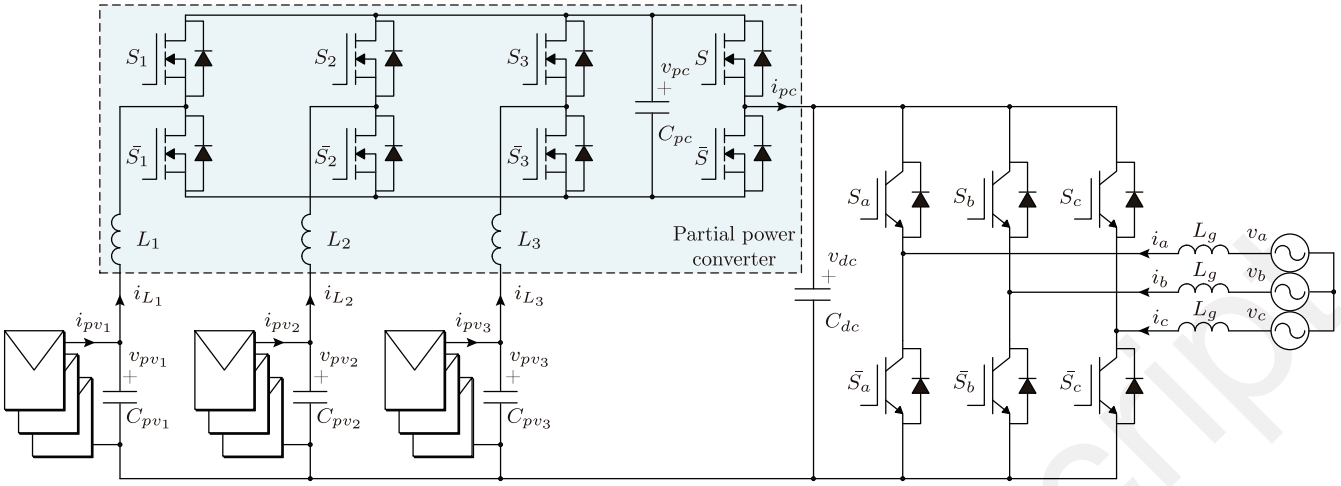


Fig. 1. Topology of the proposed partial power converter for three PV strings.

the architecture performs individual MPPT algorithm, and it allows a connection of multiple PV strings whether the application requires a high power level. In order to evaluate the architecture, three PV strings were used in this work. From the figure, it is possible to see that each leg handles the current delivered by each PV string, but the voltage is imposed by the floating capacitor. Therefore, the partial behavior is defined by the ratio between the voltage $v_{pc}$ and the input voltage $v_{pv}$, hence the power handled by the converter can be as small as the ratio is. However, the floating capacitor should ensure the operation of the converter under current variations of each string.

### B. Operational principle

In order to explain the behavior of the converter, only one PV string is considered as shown in Fig. 2. The converter works switching a pair of semiconductors, in each half-bridge one of the mosfets remains open while the other is closed. In Fig. 2 (a) when ($S_1 = 1, \bar{S} = 1$), the current $i_{L_1}$ charges the capacitor $C_{pc}$ increasing the voltage $v_{pc}$. When ($\bar{S}_1 = 1, S = 1$) as shown in Fig. 2 (b), the current $i_{L_1}$ which flows trough the capacitor discharge $C_{pc}$ decreasing the voltage $v_{pc}$. Finally, when ($S_1 = 1, S = 1$ or $\bar{S}_1 = 1, \bar{S} = 1$) as shown in Figs. 2 (c) and (d), the converter behaves as a bypass and the current $i_{L_1}$ flows without passing through the capacitor hence, the voltage $v_{pc}$ remains constant.

### C. Floating capacitor sizing

The converter voltage $v_{pc}$ must be lower than the total input voltage in order to be considered as a partial power converter. The capacitor $C_{dc}$ should be high enough to remain a constant voltage value, especially in the transitions of the MPPT algorithm because of the presence of peak currents. The capacitor voltage depends on the time of charge, and the input current hence, the maximum capacitor voltage is obtained by the following equation,

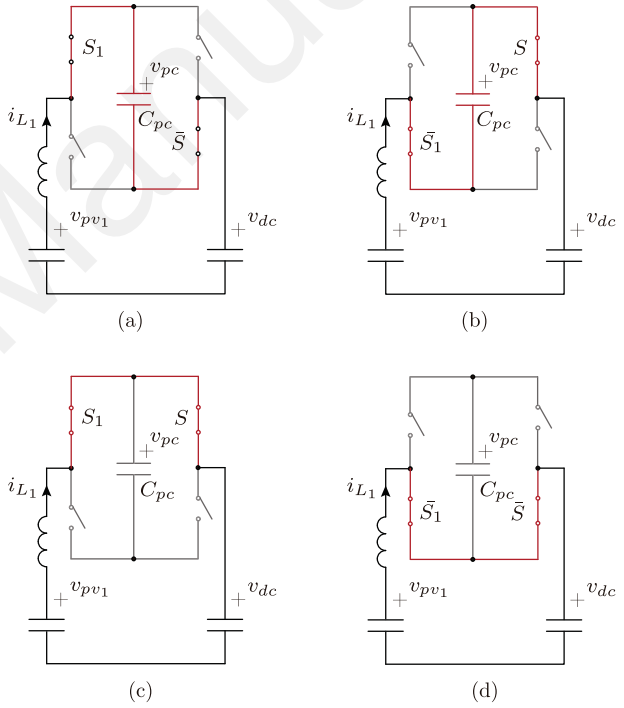


Fig. 2. Operational principle of the proposed converter. (a) $S_1 = 1, \bar{S} = 1$. (b) $\bar{S}_1 = 1, S = 1$. (c) $S_1 = 1, S = 1$. (d) $\bar{S}_1 = 1, \bar{S} = 1$.

$$V_{pc} = V_{pco} + \frac{I_{pc}}{C_{pc}} t_c - N \frac{C_{pv}}{C_{pc}} V_{pv}, \tag{2}$$

where,
$V_{pc}$: Partial converter voltage.
$V_{pco}$: Partial converter voltage at initial conditions.
$I_{pc}$: Maximum current delivered by the PV system.
$t_c$: Time of charge of the capacitor $C_{pc}$.

$N$: Number of PV strings.

The converter voltage is obtained by means of (2). However, it is possible to rearrange the equation such a way that the capacitor value could be obtained depending on the desired voltage in the converter.

$$C_{pc} = \frac{(I_{pc}t_c - NC_{pv}V_{pv})}{V_{pc} - V_{pco}}, \tag{3}$$

The initial operation procedure will be explained in the following section.

## IV. Control algorithm

### A. Control scheme

The main objective of the converter is perform an independent MPPT algorithm keeping a balanced voltage in the capacitor. The proposed control scheme is shown in Fig. 3 and it is applied for each PV string. In order to extract the maximum power, a Perturb and Observe (P&O) MPPT algorithm is performed because of the simple implementation and effective tracking [2]. It gives the voltage reference $v^*_{pv_n}$, which is controlled by an external PI controller. The output of the PV voltage control gives the current reference $i^*_{C_{pv_n}}$, which is compensated in order to obtain the current $i_{L_n}$ value. Notice that each PV string works with the same capacitor $C_{pc}$ and their half-bridge. Therefore, in order to reduce the coupling between all the currents $i_{L_n}$ an ac-component is injected. The output signal, which represents the mean value of the current $|i_{L_n}|$, is multiplied by a sinusoidal reference which has a phase delay depending on the number of PV strings. The output signal represents the current reference $i^*_{L_n}$, which is controlled by an internal PR controller with the resonance fixed at the frequency imposed by the sinusoidal reference. The signal given by the controller represents the duty cycle, but notice that it is important to avoid that the capacitor voltage $V_{pc}$ reaches a high or a zero value. Therefore, a duty cycle compensator is included which improves the $v_{pc}$ behavior under dynamic changes between the PV strings. Finally, the duty cycle reference $d^*$ goes to a classical level-shifted PWM (LS-PWM) algorithm, which gives the required signals to drive the converter.

The grid tied inverter is controlled through classical voltage oriented control (VOC) algorithm [12]. It controls the DC-link voltage for a given reference, performs grid synchronization and active and reactive power control. However, the DC-link voltage is controlled in order to balance the energy, which means a zero power consumption by the converter. Such a way, the voltage $v_{pc}$ remains in a fixed value in stationary state, and it varies when irradiation changes affect each PV string. The DC-voltage reference comes from the following equation,

$$v^*_{dc} = \frac{\sum_1^n P_n}{\sum_1^n I_{pv_n}}, n = 1, 2, 3, \tag{4}$$

where $P_n$ and $I_{pv_n}$ are the total power and the PV current delivered per each PV string.

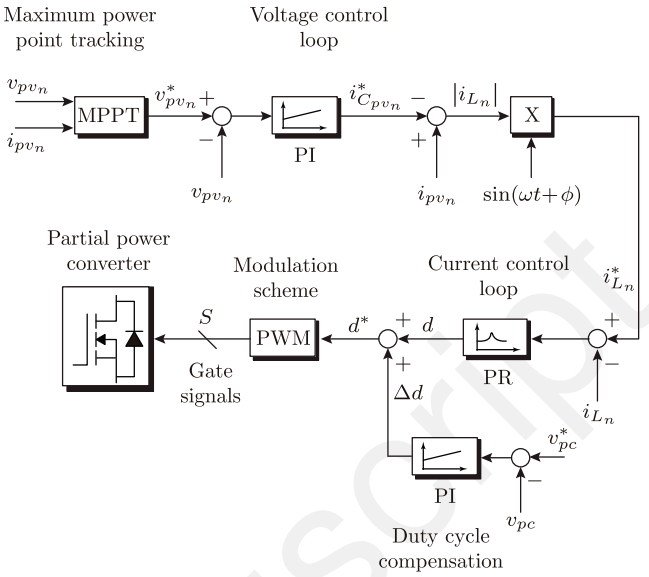


Fig. 3. DC-DC control scheme.

### B. Start-up procedure

In order to fix the initial voltage in the floating capacitor $V_{pc}$, the following procedure is implemented:

- First, a DC-link voltage is fixed at a value while ($\bar{S}_1 = 1, \bar{S} = 1$). In that way, the voltage of each PV string increases working with the maximum current.
- Once the PV strings reach a desired voltage, the control scheme is activated keeping a fixed value in the DC-link. In that way, the current will flow through the capacitor increasing the voltage $v_{pc}$. The time while this step is working will define the maximum voltage in the floating capacitor.
- Finally, with the voltage $v_{pc}$ fixed in a desired value, lower than the voltage of the PV strings, the reference for the DC-link is given according to (4).

### C. Modulation scheme

The duty cycle reference $d^*$ takes values from [-1;+1]. When the reference takes negative values, the converter controls the voltage in the capacitor $C_{pc}$ and, when the reference is positive, the converter controls the voltage in order to perform the MPPT algorithm. The proposed modulation scheme is the classical LS-PWM strategy as shown in Fig. 4. The logic of the algorithm is explained as follows:

- If the reference is above both carriers, the semiconductors of each PV string $S_n$ ($n = \{1, 2, 3\}$) operate, and the switch of the converter $S$ is turned off.
- If the reference is between both carriers, the converter behaves as bypass, it means that $S_n = S$.
- If the reference is under both carriers, the semiconductors of each PV string $S_n$ are turned off, and the switch of the converter $S$ operates.

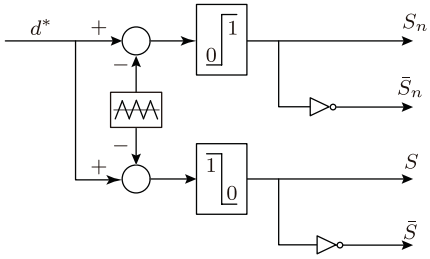


Fig. 4. Implemented modulation scheme.

## V. Simulations and Results

The validation of the proposed converter and the control schemes is performed in PLECS®. In order to reach the rated power, 34 PV panels per string and 3 strings have been used. The parameters used for the simulation are listed in the Table I. For the grid connection, a three phase H-bridge inverter is implemented.

TABLE I
Simulation Parameters

| Variable | Parameter | Value |
|---|---|---|
| $P_{pv}$ | PV power under STC | 23 KW |
| $V_{mpp}$ | Maximum PV voltage under STC | 1000 V |
| $v_g$ | Grid voltage | 380 $V_{rms}$ |
| $L$ | Filter at DC-side | 1 mH |
| $Lg$ | Filter at DC-side | 5 mH |
| $C_{pv}$ | Input capacitor | 470 $\mu$F |
| $C_{pc}$ | Capacitor of the partial converter | 15 mF |
| $C_{dc}$ | DC-link capacitor | 1000 $\mu$F |
| $f_{sw}$ | DC-DC switching frequency | 25 KHz |

The obtained results are presented in the following figures. A validation of the dynamic and independent performance is made working at different operation points. The first PV string does not present irradiation changes, it works at 1000 W/m$^2$. In the second PV string, an irradiation change to 750 W/m$^2$ is made at time t=0.75 s, and in the third PV string the irradiation change to 400 W/m$^2$ is made at time t=1.25 s.

### A. DC-side results

The first set of waveforms provided by Fig. 5 displays the voltages at the DC-side. Figs. 5 (a), (b) and (c), show the voltage evolution at each PV string respectively. The signals $v^*_{pvn}$ where $(n = \{1, 2, 3\})$, represent the voltage references in order to extract the maximum power delivered by each PV string. It can be seen how they present the typical P&O three-level waveform, and the voltage control algorithm works correctly following their respectively reference. Notice the independent MPPT algorithm and the correct response under solar irradiation changes.

Fig. 5 (d) shows the voltage $v_{pc}$, it remains constant despite of the PV voltage changes. This voltage is lower compared with the voltage at the PV side, then the power processed by the converter is lower compared with the whole power delivered by the system.

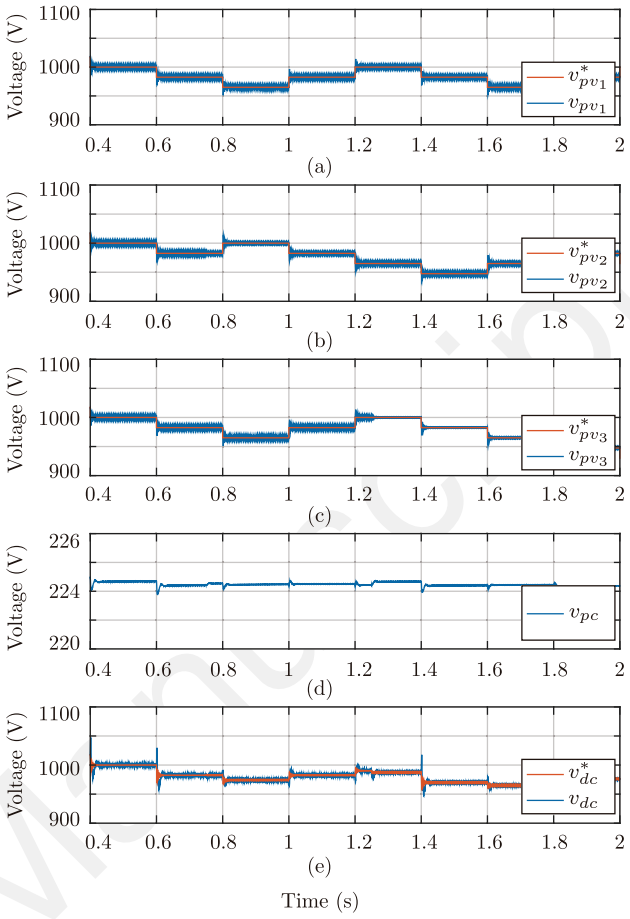


Fig. 5. Simulation results. (a) PV voltage of string 1. (b) PV voltage of string 2. (c) PV voltage of string 3. (d) Converter voltage. (e) DC-link voltage.

Fig. 5 (e) shows the voltage $v_{dc}$, it is controlled following the reference which corresponds to the energy balance equation according to (4). Notice that the application is oriented to a large-scale photovoltaic system, hence the DC-voltage is high enough to perform grid connection despite of the voltage variations derived from the solar irradiation changes.

The second set of waveforms provided by Fig. 6 displays the currents at the DC-side. Fig. 6 (a) presents the currents given by each PV string, it is possible to see the variation under different solar irradiation changes. Fig. 6 (b) presents the inductor currents, notice the AC-component imposed by the reference and the phase delay between them. The addition of these currents produces the AC-component cancellation, and the output current $i_{pc}$ shown in Fig. 6 (c), only keeps the DC-component which correspond to the total current delivered by the PV system.

### B. AC-side results and spectral distribution

The third set of waveforms displays the AC-side results and the spectral distribution of the converter currents. Figs. 7 (a) and (b) show the grid-connection, the current has a THD=4.0% and the spectral distribution is presented in Fig. 8 (a). As was

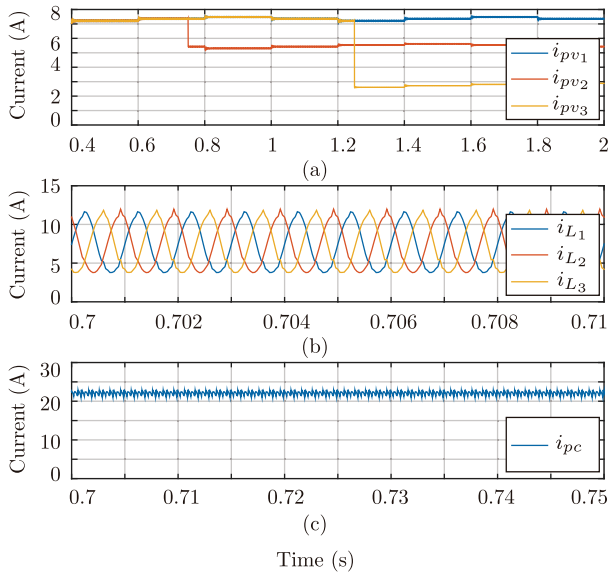


Fig. 6. Simulation results. (a) Current per PV string. (b) Current of each inductor. (c) Output current.

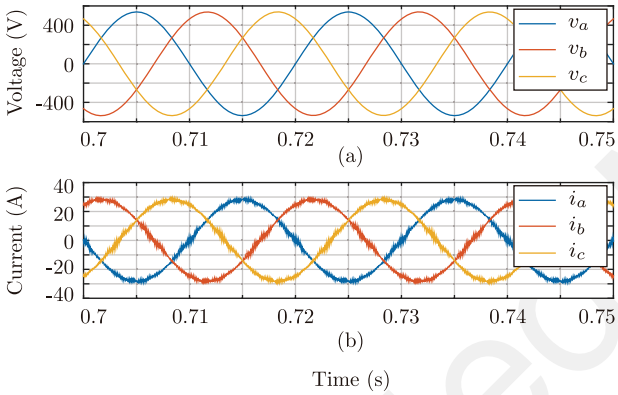


Fig. 7. Simulation results. (a) Grid voltages. (b) Grid currents.

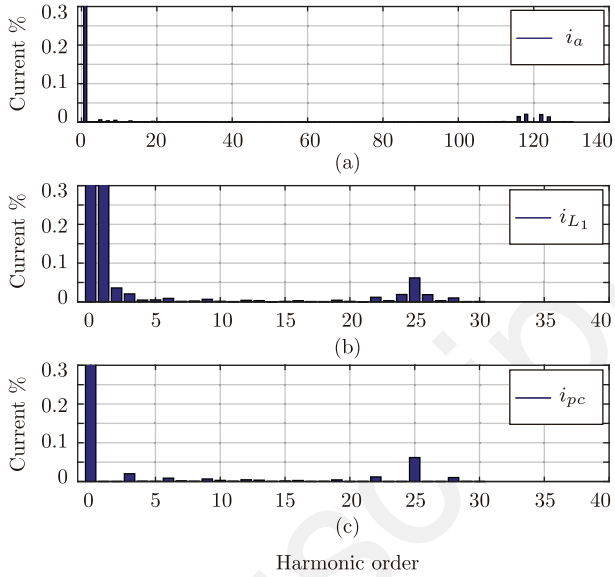


Fig. 8. Simulation results. (a) Spectral distribution for the grid current $i_a$. (b) Spectral distribution for the inductor current $i_{L_1}$. (c) Spectral distribution for the current $i_{pc}$.

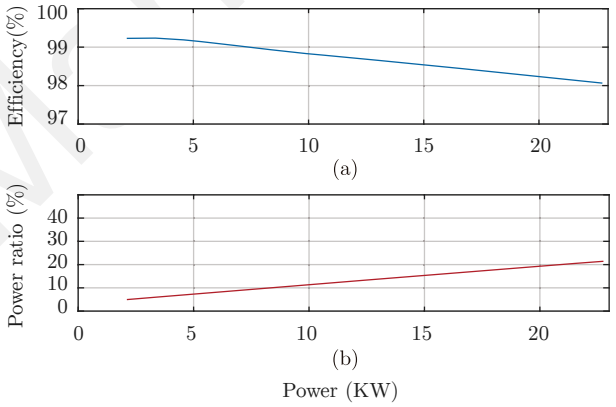


Fig. 9. Simulation results. (a) Conversion efficiency. (b) Partial power ratio $K_{pr}\%$.

mentioned before, an AC-component is imposed by the control scheme hence, the inductor currents present a DC-component, a component in the fundamental frequency and their harmonic distribution which is concentrated in the switching frequency $f_{sw}$ as shown in Fig. 8 (b). However, due to the connection, the current $i_{pc}$ only keeps the DC-component and few harmonics concentrated in the $f_{sw}$, as shown in Fig. 8 (c).

### C. Conversion efficiency

The last set of waveforms provided by Fig. 9, displays the conversion efficiency and the partial power ratio $K_{pr}\%$ under input power changes between (10-100%) of the rated power. As shown in Fig. 9 (a), the conversion efficiency (including the three phase H-bridge inverter) increases while the input power decreases because of the reduction of the switching and conduction losses. The efficiency grows until the converter stops operating due to the controller limitations. On the other hand, the power processed by the converter is reduced according to the input power reduction as shown in Fig. 9 (b). According to the results, it is possible to see that the proposed converter only process a portion of the power allowing a high conversion efficiency under different operation points.

## VI. Conclusions

The proposed topology successfully achieves partial power conversion so that the power handled is lower compared with the total power delivered by the PV system. Due to the operation principle of the converter, a series connection of PV panels is required in order to reach the input voltage needed to perform the grid-connection. Besides, due to the high input voltage and the capability of include more PV strings in

parallel connection, the proposed converter is oriented to large-scale PV systems. The individual MPPT algorithm and the reduced power processed by te converter, make the proposed architecture an attractive solution to increase the PV system efficiency.

## VII. Acknowledgment

The authors acknowledge the support provided by FONDECYT 1151426, by SERC Chile (CONICYT/FONDAP/15110019) and by AC3E (CONICYT/FB0008) of Universidad Tecnica Federico Santa Maria.

## References

[1] R. energy policy network for the 21st Century (REN21), "Renewables 2015 global status report," 2015. [Online]. Available: http://www.ren21.net

[2] S. Kouro, B. Wu, H. Abu-Rub, and F. Blaabjerg, "Chapter 7: Photovoltaic energy conversion systems," in *Power Electronics for Renewable Energy Systems, Transportation and Industrial Applications*. Wiley, 2014.

[3] N. Foureaux, A. Machado, . Silva, I. Pires, J. Brito, and B. C. F., "Central inverter topology issues in large-scale photovoltaic power plants: Shading and system losses," in *Photovoltaic Specialist Conference (PVSC), 2015 IEEE 42nd*, June 2015, pp. 1–6.

[4] S. Kouro, J. Leon, D. Vinnikov, and L. Franquelo, "Grid-connected photovoltaic systems: An overview of recent research and emerging pv converter technology," *Industrial Electronics Magazine, IEEE*, vol. 9, no. 1, pp. 47–61, March 2015.

[5] T. Esram and P. Chapman, "Comparison of photovoltaic array maximum power point tracking techniques," *Energy Conversion, IEEE Transactions on*, vol. 22, no. 2, pp. 439–449, June 2007.

[6] J. W. Zapata, S. Kouro, M. Aguirre, and T. Meynard, "Model predictive control of interleaved dc-dc stage for photovoltaic microconverters," in *Industrial Electronics Society, IECON 2015 - 41st Annual Conference of the IEEE*, Nov 2015, pp. 004 311–004 316.

[7] G. Guidi, T. M. Undeland, and Y. Hori, "An interface converter with reduced va ratings for battery-supercapacitor mixed systems," in *Power Conversion Conference - Nagoya, 2007. PCC '07*, April 2007, pp. 936–941.

[8] R. Button, "An advanced photovoltaic array regulator module," in *Energy Conversion Engineering Conference, 1996. IECEC 96., Proceedings of the 31st Intersociety*, vol. 1, Aug 1996, pp. 519–524 vol.1.

[9] A. Marzouk, S. Fournier-Bidoz, J. Yablecki, K. McLean, and O. Trescases, "Analysis of partial power processing distributed mppt for a pv powered electric aircraft," in *Power Electronics Conference (IPEC-Hiroshima 2014 - ECCE-ASIA), 2014 International*, May 2014, pp. 3496–3502.

[10] A. G. Birchenough, "A high efficiency dc bus regulator / rpc for spacecraft applications," in *Space Technology and Applications, AIP*, vol. 669, 2004, pp. 606–613.

[11] A. Morrison, J. W. Zapata, S. Kouro, M. A. Perez, T. A. Meynard, and H. Renaudineau, "Partial power dc-dc converter for photovoltaic two-stage string inverters," in *2016 IEEE Energy Conversion Congress and Exposition (ECCE)*, Sept 2016.

[12] M. Malinowski, M. P. Kazmierkowski, and A. M. Trzynadlowski, "A comparative study of control techniques for pwm rectifiers in ac adjustable speed drives," *IEEE Transactions on Power Electronics*, vol. 18, no. 6, pp. 1390–1396, Nov 2003.